Exclusive meets inclusive particle production at small Bjorken x_B: How to relate exclusive measurements to PDFs based on evolution equations

Hervé Dutrieux ,* Michael Winn ,† and Valerio Bertone ‡
IRFU, CEA, Université Paris-Saclay, 91191 Gif-sur-Yvette, France

(Received 21 February 2023; accepted 23 May 2023; published 15 June 2023)

Exclusive heavy-vector meson photoproduction is a prominent signal in collider experiments with hadron beams. At the highest photon-hadron collision energies, this process is considered as a candidate to constrain the gluon parton distribution function (PDF) at small longitudinal momentum fractions. However, in the framework of collinear factorization, exclusive particle production is described in terms of generalized parton distributions (GPDs). In this contribution, we investigate the connection between GPDs and PDFs at the leading order in α_s. Our main result is a proposal to quantify the systematic uncertainty inherent to this connection. We put our approach into context with respect to the Shuvaev transform. Our uncertainty estimate can be straightforwardly adapted to higher fixed orders and small-x resummation. The question of extrapolating GPDs to vanishing skewness is paramount for the program of the Electron Ion Collider, notably for the extraction of the radial distributions of partons.

DOI: 10.1103/PhysRevD.107.114019

I. INTRODUCTION

Partons at very small longitudinal momentum fractions and high energies constitute a particularly interesting regime of quantum chromodynamics (QCD). Gluon saturation has been predicted to occur [1]: hadrons are no longer dilute collections of partons, but interacting systems dominated by gluons. Calculations of event rates in ultra-high-energy neutrino astrophysics also depend on hadron and nuclear structure at very small longitudinal momentum fraction [2,3]. Additionally, this kinematic domain defines the initial state of the thermodynamic system created in heavy-ion and other hadron collisions at colliders [1]. It is known from experiment that gluons dominate the partonic content at small x [4,5].

However, the uncertainty on the gluon parton distribution function (PDF) for longitudinal momentum fractions $x \sim 10^{-4}$ or less is still significant. It is mostly due to a lack of experimental data in this region from deep-inelastic scattering experiments. Experimental sensitivity can nonetheless be achieved through different measurements at hadron colliders with larger collision energies $\sqrt{s}$. At the Large Hadron Collider (LHC), inclusive particle production, in particular of charm and beauty quarks, has been proposed to constrain the gluon PDF of the proton [6–10]. Although a noticeable reduction of uncertainty is produced by the inclusion of these measurements, their impact is limited by missing higher-order corrections as indicated by the large scale and hadronization uncertainties and other effects not accounted for in perturbative QCD (pQCD).

In addition to these observables, exclusive hard photoproduction processes which can also be measured at hadron colliders are relevant since they are expected to be less, or at least differently, affected by phenomena not accounted for in state-of-the-art pQCD calculations. Therefore, they have the potential to constrain PDFs at very small x, but they are not yet included in global PDF fits.

In particular, a large amount of exclusive heavy-vector meson production (HVMP) measurements of J/ψ or Υ mesons are available from the Hadron-Electron Ring Accelerator (HERA) [11–17] and from the LHC [18–23]. This already available data or future measurements produced at a possible LHeC [24] probe small values of Bjorken's x_B of the order of 10^{-4} down to 10^{-6} [25]. The future Electron Ion Collider (EIC) [26] will provide precise HVMP data with Bjorken's x_B of the order of $10^{-3} - 10^{-4}$. The leading-order (LO) two-gluon exchange in the t channel depicted in Fig. 1 is the dominant contribution to the HVMP cross section. However, because there is a transfer of four-momentum between initial- and final-state hadrons, p and p', the description of this process in the framework of collinear factorization [27] does not involve usual PDFs but the so-called generalized parton distributions (GPDs) [28–32]. Therefore, it is desirable to establish a reconstruction procedure of GPDs in the small-x region in

*herve.dutrieux@gmail.com
†michael.winn@cea.fr
‡valerio.bertone@cea.fr

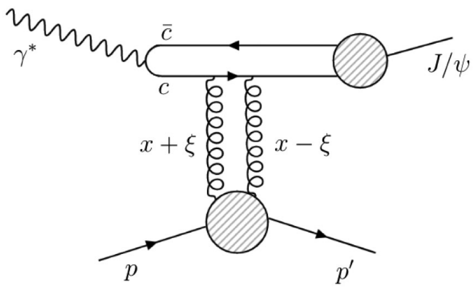

FIG. 1. Dominant contribution to the hard exclusive photoproduction of a heavy-vector meson J/ψ.

terms of PDFs. Although we stressed the practical importance of this procedure for the exploitation of HVMP data, the arguments we will develop in this paper are generically based on evolution properties of GPDs and can therefore be applied to any hard exclusive process in the regime of small Bjorken x_B. The study of the relation between GPDs and PDFs in this kinematic regime has attracted interest since the early days of GPD studies, more than two decades ago. One of the major contributions, based on the Shuvaev transform, was proposed in Refs. [33,34] and was applied to HERA and LHC experimental data for instance in Refs. [35–37]. In this article, we suggest an alternative procedure that allows us to evaluate the theoretical uncertainty associated to linking GPDs to PDFs and to pave the way for more detailed studies at higher orders and with small-x resummation.

The outline of this article is as follows. We start by exposing the problem of relating GPDs to PDFs and discuss the role of evolution. We also briefly highlight the relevance of this issue for the physics program of the EIC, independently of the question of HVMP. Next, we present our proposal to quantify the uncertainty on relating GPDs to PDFs and derive an estimate of the uncertainty for J/ψ and Υ HVMP. In the last section, we finally connect our method to the Shuvaev transform.

II. KINEMATIC VARIABLES, EVOLUTION OPERATORS, AND THE LINK BETWEEN GPDs AND PDFs

We only sketch out the properties of GPDs necessary to provide a sufficient context. More details can be found for instance in the review articles in Refs. [38–40]. We use the notation of Ref. [38] for the gluon GPD F^g. A GPD F^a for a given parton of type $a = q, g, \ldots$ in a hadron is a function of the average longitudinal momentum fraction of the parton itself, denoted by x, of the Mandelstam variable $t = (p' - p)^2$, where p and p' are the incoming and outgoing hadron four-momenta, respectively, and of the skewness ξ, which measures the longitudinal momentum transfer and can be related to Bjorken's x_B in the Bjorken limit through

$$x_B \approx \frac{2\xi}{1+\xi}. \tag{1}$$

In the following, we will use the skewness variable ξ as is customary in GPD studies, keeping in mind that in the regime of small Bjorken's x_B, $\xi \approx x_B/2$. The regime of small x_B is therefore the regime of small ξ in GPD terminology. We stress the difference between the parton longitudinal momentum fraction x, on which parton distributions depend, and Bjorken's x_B which is a kinematic variable at which an observable is measured. Many observables measured at x_B exhibit a strong sensitivity to PDFs and GPDs at values x of the order of x_B; hence, small x and small x_B are often used interchangeably. However, in general, factorized observables depend on an integral of parton distributions over a range of values of x, typically up to $x = 1$.

In addition to (x, ξ, t), GPDs also depend on a factorization scale denoted by μ. The relation between the GPD F^a and the corresponding PDF f^a for the same parton and hadron helicities in initial and final states is given by

$$F^a(x, \xi = 0, t = 0, \mu) = x^{p_a} f^a(x, \mu), \tag{2}$$

where $p_a = 0$ for quarks ($a = q$) and 1 for gluons ($a = g$). As discussed in the previous section, our main objective is to reconstruct the GPDs at small x and x_B (that is small x and ξ) from PDFs. Equation (2) gives a straightforward answer even if ξ is not strictly zero, but $x \gg \xi$ and t is negligible compared to the hard scale of the process. Then the four-momentum transfer may be neglected altogether and the GPD approximated by the PDF. If $x \gg \xi$ but t is not negligible, relating GPDs to PDFs requires control over the t behavior, usually expressed by an exponential ansatz for the t dependence as for instance in Ref. [35]. A study of the variation of the t dependence under evolution for some models can be found in Ref. [41].

Since the uncertainty on the relation between GPDs and PDFs at nonvanishing t can be adequately addressed by flexible parametrizations of the t dependence, we will set this aspect aside and focus on linking GPDs and PDFs when ξ is non-negligible as compared to x. This case deserves a particular attention for several reasons.

(1) Evolution equations produce a direct entanglement of the x, ξ, and μ, whereas the evolution kernels are independent of t.
(2) The convolution of GPDs that enters the computation of exclusive HVMP exhibits a strong sensitivity to the region $x \approx \xi$. Therefore, the region where GPDs cannot be bluntly approximated by PDFs is precisely the one that we are mostly concerned with.
(3) GPDs with vanishing skewness $F^a(x, \xi = 0, t)$ are of great importance, as they are used for the definition of impact-parameter distributions (IPDs) [42] that give the number density of a parton carrying a

fraction of longitudinal momentum x at the radial distance $b_\perp$ from the center of momentum of the hadron in the infinite momentum frame:

$$\mathrm{IPD}^a(x, b_\perp, \mu) = \int \frac{\mathrm{d}^2\Delta_\perp}{(2\pi)^2} e^{-ib_\perp\cdot\Delta_\perp} F^a \times (x, \xi = 0, t = -\Delta_\perp^2, \mu). \quad (3)$$

The imaging of the hadronic structure in position space has been identified as one of the goals of the EIC program [26]. As most data for exclusive processes are taken at nonvanishing skewness, an understanding of the uncertainty associated to the extrapolation to $\xi = 0$ at fixed values of t is crucial to this purpose and is provided by the procedure we present in this article.

Since HVMP is only sensitive to C-even GPDs, in the following we will consider only such GPDs, also known as singlet GPDs. They have a definite parity in x—gluon GPDs are x even and quark singlet GPDs are x odd—which allows us to only focus on the case where $x \geq 0$. In general, GPDs are also even functions of ξ due to time-reversal invariance, so we consider only $\xi \geq 0$ as well.

The dependence of PDFs on their scale μ is given by the Dokshitzer-Gribov-Lipatov-Altarelli-Parisi (DGLAP) equations [43–45] which ensure that observables computed from PDFs do not depend on the arbitrary scale μ. Analogously, GPDs obey their own evolution equations [28,30,32], which generalize the DGLAP equations and whose solution reads [46]

$$\frac{F^a(x, \xi, t, \mu)}{x^{p_a}} = \sum_{b=q,g,\ldots} \int_0^1 \frac{\mathrm{d}z}{x} \Gamma^{ab}\left(\frac{z}{x}, \frac{\xi}{x}; \mu_0, \mu\right) \times \frac{F^b(z, \xi, t, \mu_0)}{z^{p_b}}. \quad (4)$$

In view of the definition in Eq. (4), the solution to the DGLAP evolution equations can be written as

$$f^a(x, \mu) = \sum_{b=q,g,\ldots} \int_0^1 \frac{\mathrm{d}z}{x} \Gamma_0^{ab}\left(\frac{z}{x}; \mu_0, \mu\right) f^b(z, \mu_0), \quad (5)$$

where the DGLAP evolution operator Γ_0^{ab} is linked to the GPD one Γ^{ab} through

$$\Gamma_0^{ab}\left(\frac{z}{x}; \mu_0, \mu\right) = \lim_{\xi/x\to 0} \Gamma^{ab}\left(\frac{z}{x}, \frac{\xi}{x}; \mu_0, \mu\right). \quad (6)$$

The DGLAP operator $\Gamma_0^{ab}(z/x; \mu_0, \mu)$ takes nonzero values for $\mu \geq \mu_0$ if and only if $z \geq x$. Intuitively, this can be understood as follows: since the DGLAP evolution describes the substructure of partons as the resolution at which the system is probed increases, a parton carrying a longitudinal momentum fraction x at the initial scale radiates several partons ending up with a momentum fraction less than x at the final scale. In practice, as we will show below, DGLAP evolution, and the general GPD evolution for $x \geq \xi$ as well, pushes distributions from large to small x. As a result, the higher the evolution range, the more variations of the distribution at initial scale are washed away toward a smaller-x domain. This general idea forms the basis of the strategy to reconstruct the ξ dependence of GPDs from PDFs: we may ignore the ξ dependence of GPDs at an initial low-lying scale, but the known ξ dependence generated by evolution to sufficiently higher scales washes away this uncertainty.

Before undertaking a discussion of the ξ dependence of the LO evolution operator, it is enlightening to observe directly its consequences. In Fig. 2, we use the LO PDF set MMHT2014 [47] as an input at the scale $\mu_0 = 1$ GeV and evolve it to $\mu = 4.7$ GeV using both the ordinary LO DGLAP equation ($\xi = 0$) and the LO GPD evolution equation at $\xi = 10^{-4}$. In accordance with the MMHT2014 LO extraction, the running of the strong coupling is computed at one loop with $\alpha_s(M_Z) = 0.135$ in the variable-flavor-number scheme, with the charm threshold at 1.4 GeV. As we use the same distribution at initial scale,

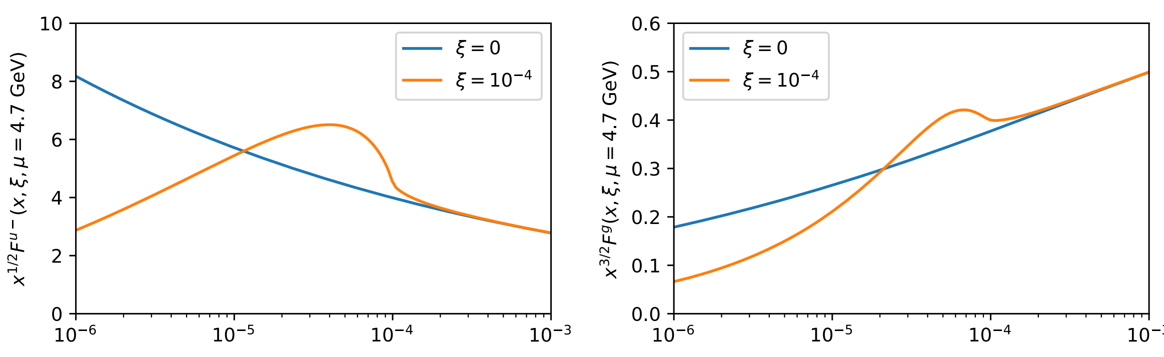

FIG. 2. Evolution of the MMHT2014 LO PDF [47] from $\mu_0 = 1$ to 4.7 GeV using the DGLAP evolution (blue curve) and the GPD evolution at $\xi = 10^{-4}$ (orange curve). On the left, we show the nonsinglet u PDF defined by $u^-(x) = u(x) - \bar{u}(x)$. On the right, the gluon PDF. The difference between the two curves becomes sizable for $x \lesssim 3\xi$.

the entire difference between the curves in Fig. 2 is due to the ξ dependence introduced by the evolution operator. One can observe immediately that the difference is only perceptible for $x \lesssim 3\xi$. As we have already mentioned, this is the region of largest phenomenological interest for the description of HVMP data.

Referring to Eq. (4), the Γ^{ab} operators give a weighting [48] of GPDs at the initial scale μ_0 to produce GPDs at the final scale μ. As such, they allow one to gauge the importance of the contribution to the evolution of various regions of the GPDs at the initial scale. The properties of the evolution at small values of ξ have notably been studied in Refs. [34,41,49,50] but, to the best of our knowledge, studies of this kind have been performed by means of models of GPDs, often with the assumption of power-law behavior at small x, and have therefore a lesser generality than our discussion which takes place directly at the level of the Γ^{ab} operators. We use the GPD evolution software APFEL++ [51–53] to numerically study their properties. For numerical applications, we will use the typical hard scales encountered in HVMP, given by half the mass of the vector meson as argued in Refs. [54,55], that is $\mu_c = m_{J/\psi}/2 = 1.5$ GeV and $\mu_b = m_\Upsilon/2 = 4.7$ GeV. Since we only perform LO evolution, we need an initial evolution scale high enough to produce coherent results. We choose as an initial scale $\mu_0 = 1$ GeV and plot in Fig. 3 the evolution operators $\Gamma^{ab}(z/x, \xi/x; \mu_0, \mu)$ as functions of z/x evaluated at $\mu = \mu_c$ and μ_b in the variable-flavor-number scheme, using $\alpha_s(M_Z) = 0.118$ as a boundary condition for the evolution of the strong coupling. Let us comment on some important aspects.

(1) We only focus on the case $\xi \leq x$ [56]. A specific procedure, called covariant extension [57,58], allows one to retrieve the $\xi > x$ region from the $\xi \leq x$ one, up to a specific function known as the D term. Since the D term only lives in the region $\xi > x$ and enjoys its own independent evolution equation, it does not provide any handle on PDFs. Therefore, the D-term contribution to the amplitude of a process, which can be isolated in the formalism of dispersion relations (see for instance Refs. [59,60]), is ignored in the present study. The region $\xi \leq x$ possesses another important property: $F^a(x, \xi, t, \mu)$ only depends on values of $F^b(z, \xi, t, \mu_0)$ such that $z \geq x$, as can be observed in Fig. 3. We have already mentioned this property in the case of the DGLAP operator ($\xi = 0$).

(2) The qq and gg sectors exhibit a strong peak at $z = x$, all the more that μ is close to μ_0. This is easily understandable because in the limit of no evolution, where $\mu = \mu_0$, $\Gamma^{ab}(z/x, \xi/x; \mu_0, \mu_0) = \delta_{a,b}\delta(1 - z/x)$ where $\delta_{a,b}$ is the Kronecker delta. On the contrary, as μ increases the contribution from the region $z \gg x$

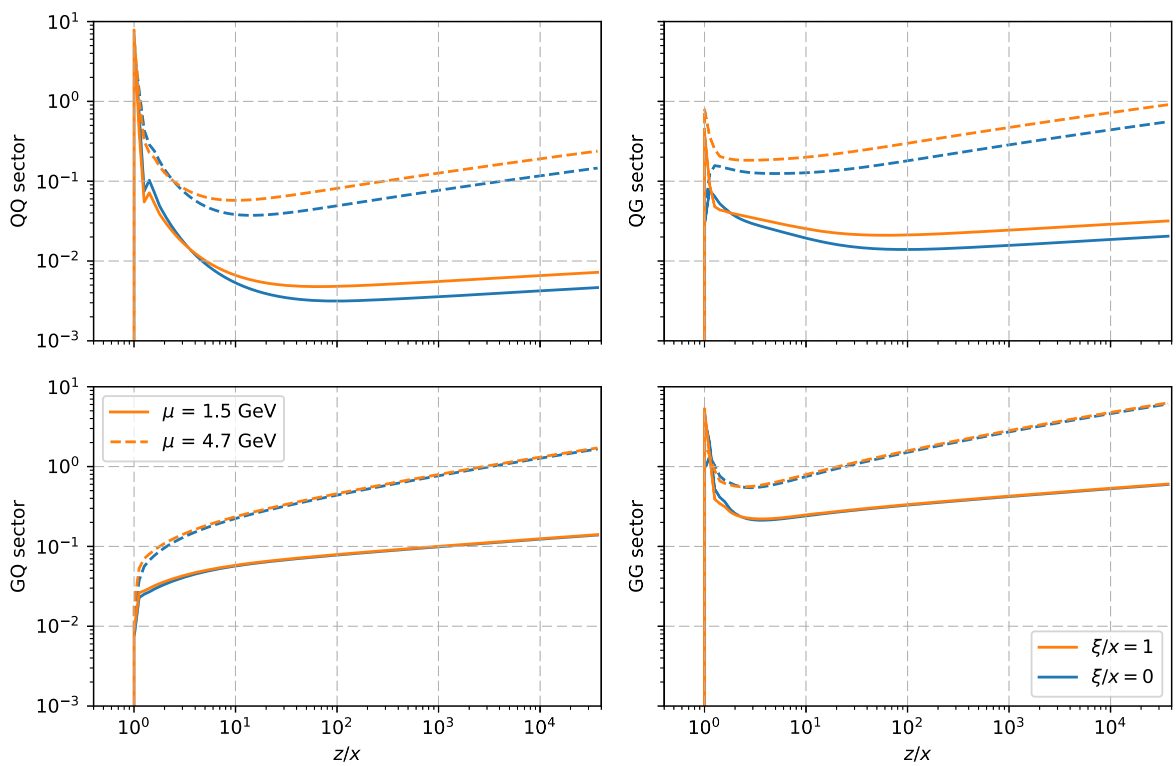

FIG. 3. Behavior of $\Gamma^{ab}(z/x, \xi/x; \mu_0 = 1$ GeV$, \mu)$ in the four sectors $ab = qq$ (upper left), $ab = qg$ (upper right), $ab = gq$ (lower left) and $ab = gg$ (lower left). The continuous lines stand for the final scale $\mu = m_{J/\psi}/2 = 1.5$ GeV while the dotted lines for $\mu = m_\Upsilon/2 = 4.7$ GeV. The colors refer to the value of the ratio ξ/x: $\xi = 0$ is the DGLAP operator (blue) and $x = \xi$ is in orange.

becomes increasingly important. This corresponds to a kinematic region where at the initial scale μ_0 the asymmetry between the four-momenta of incoming and outgoing active parton, $z+\xi$ and $z-\xi$, is negligible and the GPDs can safely be replaced by the PDFs. The fact that this region becomes increasingly dominant as evolution to higher and higher scale is performed provides a quantitative argument that the evolution washes away the uncertainty on the ξ behavior of the GPDs at the initial scale. As the behavior of the evolved GPDs is increasingly controlled by its large-z region at the initial scale, the initial uncertainty on their ξ dependence becomes negligible.

(3) Finally, one can observe that the DGLAP operator ($\xi = 0$) and the GPD evolution operator at $x = \xi$ share a globally similar shape. Nonetheless, the curves in the gg and gq sectors, which seem almost identical for $z/x \gtrsim 5$, actually differ by an almost constant factor of 5% between $\xi = x$ and $\xi = 0$ in the large z/x domain at $\mu = 4.7$ GeV. The difference is much starker in the qq and qg sectors, with an almost constant factor of 50% for the same parameters. Significant differences are furthermore observed in the region where z is of the order of x. This explains why in Fig. 2 the GPD evolution at $\xi = 10^{-4}$ produces larger values than the DGLAP evolution around $x = \xi$. The fact that the region around $x = \xi$ would evolve faster than the PDF was already identified in a number of early references [34,49,61] and often taken into account in models with the help of an appropriately tuned "skewness ratio" $F^a(x, \xi = x)/F^a(x, \xi = 0)$.

Let us now draw a few conclusions. From Figs. 2 and 3, it is clear that simply using PDFs instead of GPDs when $x \approx \xi$ brings potential GPD modeling uncertainties of the order of several tens of percent even when ξ is arbitrarily small. The skewness ratios quoted in Refs. [34,49] reach in some cases even higher values where GPDs at $x = \xi$ are about 1.6 times as large as the corresponding PDFs. A precise study of HVMP must deal with this source of uncertainty. A path to do so is already clear. At a very low scales, the ξ dependence of a GPD may be unknown, but as the GPD is evolved, the increasing dominance of the region $z \gg \xi$ allows for a reduction of the uncertainty. This handle on the uncertainty of the extrapolation to zero skewness will depend on the range in μ, the value of ξ and the x profile of the GPD at the initial scale. With this in mind, we can lay down our proposal to relate GPDs to PDFs with a quantification of systematic uncertainties.

III. PROPOSAL TO QUANTIFY THE SYSTEMATIC UNCERTAINTY IN RELATING GPDs TO PDFs

The model of reconstruction of the ξ dependence of GPDs at small ξ that we suggest is straightforward: we simply propose to approximate the GPDs by the PDFs at the low scale μ_0. Then we evolve them to the hard scale μ with the full ξ-dependent GPD evolution operator. Observables can then be computed with this object whose entire ξ dependence has been generated by evolution. We will show in the next section that this model is conceptually close to the one based on the Shuvaev transform, although with notable differences.

Beyond its simplicity, the main advantage of our proposal is the possibility to compute an estimate of the associated systematic uncertainty. Since we don't know the ξ dependence of the GPDs at the initial scale, there is by definition a certain level of arbitrariness in any attempt to quantify the uncertainty of our procedure, which can be used as a conservative estimate of the magnitude of the uncertainty. At the initial scale μ_0, pessimistic estimates derived from the skewness ratio evoked at the end of the previous section lead us to assume a plausible uncertainty of up to 60% at $z = \xi$ between the GPD $F^a(z = \xi, \xi, \mu_0)$ and the PDF $f^a(z, \mu_0)$. We expect this uncertainty to decrease quickly as z increases and become essentially negligible for $z \gtrsim 10\xi$. We show in Fig. 4 two plausible profiles of uncertainty on the ξ dependence of the GPD at the initial scale as a function of z/ξ, given by

$$\eta\left(\frac{z}{\xi}\right) = 0.6 \exp\left(\frac{\xi - z}{\alpha\xi}\right), \tag{7}$$

with $\alpha = 1$ to simulate a fast decrease in uncertainty and $\alpha = 2$ for a slower decrease. As we will see, this does not make much difference, indicating that it is the uncertainty at $z = \xi$ which represents the most critical source of uncertainty.

Then we assume $\eta(z/\xi) f^a(z, \mu_0)$ to be an upper bound on the uncertainty of the GPD at initial scale, and we can

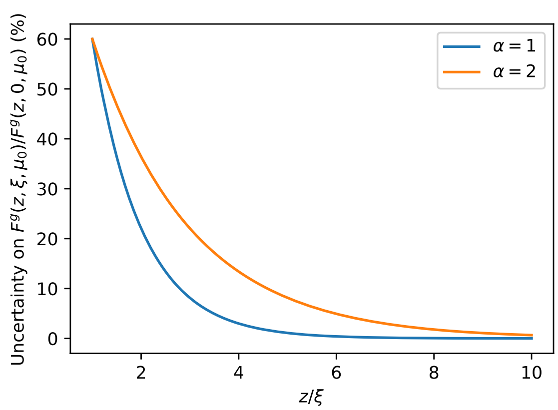

FIG. 4. Uncertainty profiles produced by Eq. (7) with $\alpha = 1$ (blue curve) and $\alpha = 2$ (orange curve) to quantify the unknown ξ dependence of the GPDs at the initial scale. In both cases, we assume that the GPD at $\xi = z$ deviates by 60% from the corresponding PDF. For $z \gtrsim 10\xi$, the difference between PDF and GPD is very small as one would expect.

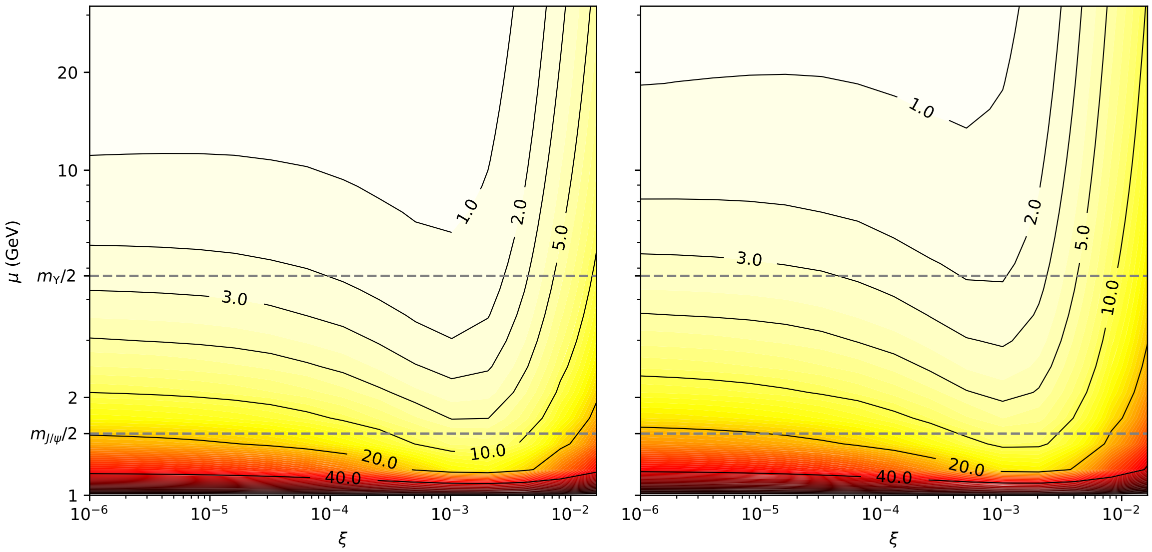

FIG. 5. Behavior of $\Delta^g(x = \xi, \xi, \mu)$ in percent as a function of ξ and μ for the LO PDF set MMHT2014 used as input at the scale $\mu_0 = 1$ GeV. On the left, we use the uncertainty profile with $\alpha = 1$ while on the right with $\alpha = 2$ [see Fig. 4 and Eq. (7)].

define our conservative magnitude of uncertainty at scale μ by simply integrating this uncertainty against the evolution operators:

$$\Delta^a(x,\xi,\mu) = \frac{\sum_b \int_0^1 \frac{dz}{x} \Gamma^{ab}\left(\frac{z}{x}, \frac{\xi}{x}; \mu_0, \mu\right) \eta(\frac{z}{\xi}) f^b(z,\mu_0)}{\sum_b \int_0^1 \frac{dz}{x} \Gamma^{ab}\left(\frac{z}{x}, \frac{\xi}{x}; \mu_0, \mu\right) f^b(z,\mu_0)}. \quad (8)$$

For instance, if $\mu = \mu_0$, which corresponds to no evolution, then the relevant evolution operators are just Dirac peaks centered at $x = z$, and

$$\Delta^a(x,\xi,\mu=\mu_0) = \frac{\sum_b \delta_{a,b} \eta(x/\xi) f^b(x,\mu_0)}{\sum_b \delta_{a,b} f^b(x,\mu_0)} = \eta\left(\frac{x}{\xi}\right). \quad (9)$$

As expected, without evolution we recover exactly the uncertainty assumed at the initial scale given by the function η.

We display in Fig. 5 the behavior of $\Delta^g(x = \xi, \mu)$ for the LO PDF set MMHT2014 [47] as an input at $\mu_0 = 1$ GeV. On the left, Δ^g is represented with an uncertainty at initial scale produced by the function η with parameter $\alpha = 1$. As compared to the case on the right where $\alpha = 2$, this corresponds to significantly smaller uncertainties for $z > \xi$. Yet, the results are similar, proving that the determining source of uncertainty comes from the region around $z = \xi$.

As expected from Eq. (9), when μ is very small, the uncertainty is close to $\eta(1) = 60\%$. At the scale $\mu = 1.5$ GeV, corresponding to J/ψ production, the uncertainty of the ξ reconstruction of the gluon GPD can be estimated to be 10%–20% for a large range of values of ξ. At the scale $\mu = 4.7$ GeV corresponding to Υ production, the uncertainty on the gluon GPD drops approximately to 2%–4%. Although at LO HVMP is only sensitive to the gluon GPD, we show the result for the light quark sea GPD in Fig. 6. There the situation is much more dire, with an uncertainty of order 40% for J/ψ production and 10% for Υ. This is easily understood by looking at the evolution operators shown in Fig. 3. The contribution of the large-z region for the qq operator is significantly less than that of the gg operator, meaning that the effect of washing away of uncertainty by evolution is much less effective for quarks than for gluons.

The behavior of Δ^g as a function of ξ results from two opposite trends. When ξ is still rather large, the decrease of ξ triggers a very quick increase of the contribution of the region $z \gg \xi$, resulting in a quick reduction of the uncertainty. However, when ξ decreases below roughly 10^{-3}, Δ^g stabilizes. The cause of this behavior is an interplay between the increase of the operator weights Γ^{ab} in the large-z region and the steep increase of the PDFs themselves at small z. As a consequence, the power-law behavior of the PDFs at small z stabilizes the dominance of the large-z region in the evolution. Rather than ξ, it is μ which plays the most important role in the quality of the approximation.

We believe that one can use the value of $\Delta^a(x, \xi, \mu)$ as a conservative estimate of the uncertainty generated by the extrapolation to vanishing skewness of GPDs. As mentioned in the previous section, the extrapolation to $\xi \to 0$ is not only relevant to relate GPDs to PDFs in the context of small-x HVMP, but also to the extraction of IPDs (3), a major aspect of the hadron tomography program.

The uncertainty in the extrapolation to vanishing skewness depends on three aspects: the choice of the low-lying scale μ_0, the choice of the uncertainty profile η (7), and the knowledge of the PDFs at the initial scale μ_0. Let us review them one by one. Since we are using a perturbative

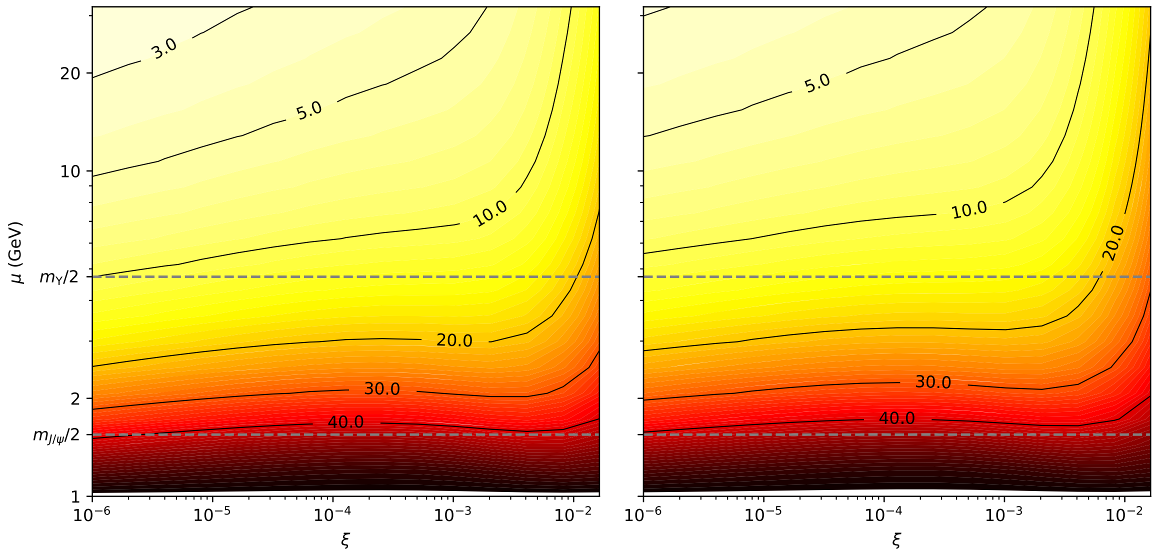

FIG. 6. Behavior of $\Delta^q(x = \xi, \xi, \mu)$ in percent as a function of ξ and μ for the LO PDF set MMHT2014 used as input at the scale $\mu_0 = 1$ GeV. On the left, we use the uncertainty profile with $\alpha = 1$ while on the right with $\alpha = 2$ [see Fig. 4 and Eq. (7)].

generation of the ξ dependence, it is in our best interest to define μ_0 as low as possible to increase the leverage of evolution, which we have highlighted in Fig. 5 to be a dominant factor in the reduction of Δ^a. However, μ_0 is bound from below by the shortcomings of perturbation theory at small scale. Determining the smallest scale which allows the use of perturbation arguments presents a level of arbitrariness. However it makes a crucial difference in the evaluation of the uncertainty as the strongest evolution effects precisely happen at small scale. To give a sense of the dependence on the choice of μ_0, we reproduce the left plot of Fig. 5 starting now from $\mu_0 = 1.4$ GeV in Fig. 7 instead of 1 GeV. We still assume 60% of uncertainty at the new value of μ_0 with the same appropriately evolved model of PDF. With such choice of starting scale, the formalism is now not applicable to the J/ψ production if the hard scale $m_{J/\psi}/2$ is used as argued in Refs. [54,55]. Indeed, since the hard scale almost corresponds to our starting scale, we recover about 60% of uncertainty. On the other hand, for Υ production at a hard scale $m_\Upsilon/2$, the value of Δ^g has now increased to 3%–8% on a wide range of ξ, compared to the values 2%–4% we had quoted before. The general features of the (μ, ξ) dependence of Δ^a remain the same.

That Δ^a depends on the choice of uncertainty profile (7) is the consequence of the fact that we are trying to quantify something that is fundamentally unknown, namely the ξ dependence of GPDs at the low-lying scale μ_0. Figure 5 highlights that a dominant factor in the uncertainty profile is $\eta(1)$, which characterizes the difference between $F^a(x = \xi, \mu_0)$ and $f^a(x, \mu_0)$. In this study, we have used $\eta(1) = 60\%$ based on a general argument of large skewness ratios encountered in the literature, but it unfortunately boils down to the physicist to make an assumption on the bound of "reasonable" uncertainties on the GPDs at the initial

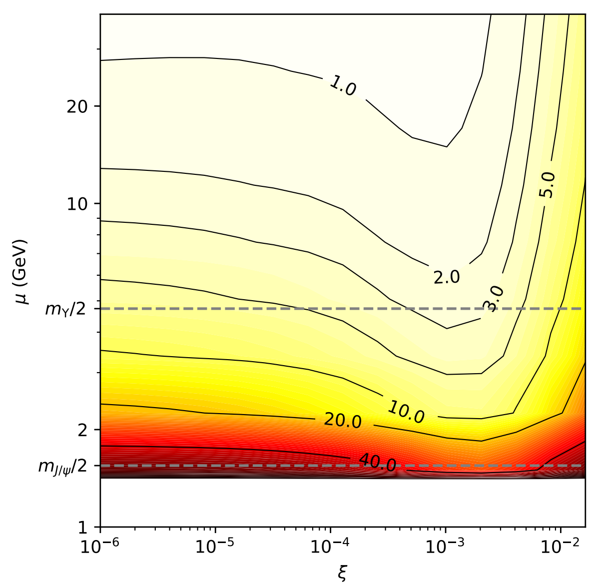

FIG. 7. Behavior of $\Delta^g(x = \xi, \xi, \mu)$ in percent as a function of ξ and μ for the LO PDF set MMHT2014 used as input at the scale $\mu_0 = 1.4$ GeV with uncertainty profile characterized by $\alpha = 1$. Compare to the left-hand side plot of Fig. 5 where $\mu_0 = 1$ GeV.

scale. It is obvious that an arbitrarily large uncertainty at initial scale μ_0 would result in an arbitrarily large uncertainty at a hard scale as well.

Finally, Δ^a depends on the PDF profile at μ_0. It means that our uncertainty estimate is Bayesian in nature, in the sense that the uncertainty in relating the GPDs to the PDFs at the hard scale μ depends on our prior knowledge of the PDFs at the scale μ_0. This can be understood physically: if the PDFs at the low scale μ_0 increase only moderately at small x, then the dominance of the large-z region is easier to establish, and the uncertainty Δ^a is smaller. The uncertainty Δ^a should therefore be evaluated with respect to our current best knowledge of PDFs at small x and low scales. To fully leverage the Bayesian viewpoint on the uncertainty of the vanishing ξ extrapolation, one could consider the following strategy:

(1) Start from the current best knowledge of PDFs at the low scale μ_0.
(2) Evolve this PDF set using ξ-dependent GPD evolution to the hard scale of the process. This produces GPD-like objects with a ξ dependence entirely resulting from evolution. The set of GPD-like objects inherits the uncertainty of the initial PDF set. It must further be smeared by Δ^a defined in Eq. (8) to take into account the uncertainty due to the unknown ξ dependence of the GPD at initial scale.
(3) The set of GPD-like objects now constitutes a Bayesian prior on the GPD at the relevant hard scale, with an account of systematic uncertainty. Traditional Bayesian inference techniques can then be used to update this prior knowledge with new information coming from actual HVMP data or any other exclusive process. For instance, if the knowledge of PDFs is represented by samples (e.g. from a neural network model), Bayesian reweighting assigns a likelihood coefficient to each sample of the PDF set by comparing the prediction using the prior GPD-like objects to the actual measurements. This allows HVMP to update the knowledge of the PDF while taking into account the previous uncertainty of PDFs, the uncertainty on the ξ dependence and the experimental uncertainty of the HVMP data.

Reweighting strategies as described in the last step are a well-established technique for PDFs and are increasingly used for higher-dimensional parton distributions (see for instance Refs. [62–64]). The Bayesian technique offers additionally the advantage of possibly highlighting signs of an interesting physics (for instance, the need to take into account effects of small-x resummation) by a significant tension between the observables computed from the GPD-like prior and the actual measurements. However, to conclude that such tensions result from an inability of the ordinary collinear framework to accommodate the data, one would need a careful control of the biases in the initial PDF parametrization. Indeed, the procedure we suggest is only as good as the modeling of the initial knowledge of the PDF itself, as well as the t dependence, that we do not try to address in this paper. In the absence of a good flexible parametrization of the PDF, a more rudimentary approach would simply consist in adding Δ^a as a general systematic uncertainty to the relation of GPD to PDF. One could further compare Δ^a computed using alternatively the collinear evolution kernel as we have done here or including small-x resummation in the spirit of various attempts to modify the DGLAP equation in the small-x region (see for instance Ref. [65] and references therein). Using higher-order perturbative evolution would also be desirable to reduce missing higher-order corrections, which become all the more sizable that the initial scale is low.

The proposal we have developed in this section is similar in its general strategy to the one based on the Shuvaev transformed which was already applied for instance in Refs. [35–37]. We clarify in the next section how the two modeling strategies differ.

IV. REVISITING THE MODELING OF GPDs THROUGH THE SHUVAEV TRANSFORM

The Shuvaev transform [33,34] relates the representation of GPDs in momentum space as we presented them so far to the representation of GPDs in the space of conformal moments. Conformal moments are defined as [38]

$$\mathcal{O}_n^a(\xi,t,\mu) = \frac{\Gamma(n+1-p_a)\Gamma(p_a+3/2)}{2^{n-p_a}\Gamma(n+3/2)} \times \xi^{n-p_a}\int_{-1}^{1}\mathrm{d}x C_{n-p_a}^{(p_a+3/2)}\left(\frac{x}{\xi}\right)F^a(x,\xi,t,\mu), \tag{10}$$

where $C_n^{(p_a+3/2)}$ are Gegenbauer polynomials and Γ is the Euler gamma function generalizing factorials. The prefactor with Γ functions is introduced such that in the limit $t=0$ and $\xi=0$, the conformal moments are exactly equal to the Mellin moments of the PDF, defined by

$$\mathcal{M}_n^a(\mu) = \int_{-1}^{1}\mathrm{d}x x^n f^a(x,\mu). \tag{11}$$

Conformal moments are particularly suitable to solve the LO GPD evolution equations [66,67]. For instance, for n even—that corresponds to the quark nonsinglet GPD—the ξ and μ dependence is factorized as follows:

$$\mathcal{O}_n^q(\xi,t,\mu) = \mathcal{O}_n^q(\xi,t,\mu_0)\left(\frac{\alpha_s(\mu)}{\alpha_s(\mu_0)}\right)^{\gamma_n/2\beta_0}, \tag{12}$$

where the anomalous dimensions γ_n are the same as those that govern the DGLAP evolution of PDFs. In the singlet case, only conformal moments associated to the same odd value of n mix between the gluon and quark singlet GPDs. The Shuvaev operator, which we denote as $\mathcal{S}^a(x,\xi;n)$, allows one to relate the two representations of GPDs through

$$F^a(x,\xi,t,\mu) = \mathcal{S}^a(x,\xi,n) * \mathcal{O}_n^a(\xi,t,\mu), \tag{13}$$

where we use the $*$ notation to indicate the action of the Shuvaev operator on an analytical continuation of the conformal moments.

Defining the ξ dependence of GPDs can equivalently take the form of defining the ξ dependence of conformal moments. The modeling proposal of GPDs at small ξ based on the Shuvaev transform consists in approximating the conformal moments in the limit $\xi \ll 1$ with their value at $\xi = 0$, i.e. in defining a GPD model whose conformal moments are constant in ξ and equal to

$$\mathcal{O}_n^a(\xi, t, \mu) \equiv \int_{-1}^{1} \mathrm{d}x x^{n-p_a} F^a(x, \xi = 0, t, \mu), \qquad \xi \ll 1, \tag{14}$$

which are exactly the Mellin moments of the PDF if $t = 0$. We will again set aside the question of the modeling of the t dependence, which should ideally be the subject of a flexible parametrization at the level of conformal moments. At $t = 0$, this model greatly simplifies the expression of Eq. (13), since it can be turned into the following form:

$$F^a(x, \xi, \mu) \equiv \mathcal{S}'^a(x, \xi, \mathbf{x}') * f^a(\mathbf{x}', \mu), \tag{15}$$

where $\mathcal{S}'^a$ is now the composition of the Shuvaev operator $\mathcal{S}^a$ and the Mellin transform (see the Appendix for details). We use the boldface character $\mathbf{x}'$ so that no ambiguity arises on the actual integration variable subtended by the symbol $*$. An equivalent formalism related to the assumption of ξ independence of conformal moments has been discussed in Ref. [61]. The proposal has been extended in Ref. [68], which provides a technical fix so that the reconstructed GPDs do not extend outside the physical support $x \in [-1, 1]$.

Let us show how this modeling (ξ-independent conformal moments) is deeply related to the one we presented in the previous section (GPD = PDF at a low scale μ_0 and ξ-dependent evolution applied to reach μ). First we note the following remarkable property linking the DGLAP LO evolution operators Γ_0^{ab} introduced in Eq. (5) to the general LO evolution operators defined in Eq. (4): provided $z \gg \xi$, and given any $\mu > \mu_0$,

$$\frac{1}{x}\Gamma^{ab}\left(\frac{z}{\xi}, \frac{\xi}{x}; \mu_0, \mu\right) \approx \frac{1}{x^{p_a}} \mathcal{S}'^a(x, \xi, \mathbf{x}') * \frac{1}{\mathbf{x}'}\Gamma_0^{ab}\left(\frac{z}{\mathbf{x}'}; \mu_0, \mu\right). \tag{16}$$

In other words, in the limit where $z \gg \xi$, the ξ dependence of the general LO evolution operator can be entirely reproduced by the ξ dependence of S'. Figure 8 shows the excellent quality of this approximation in the qq and gg

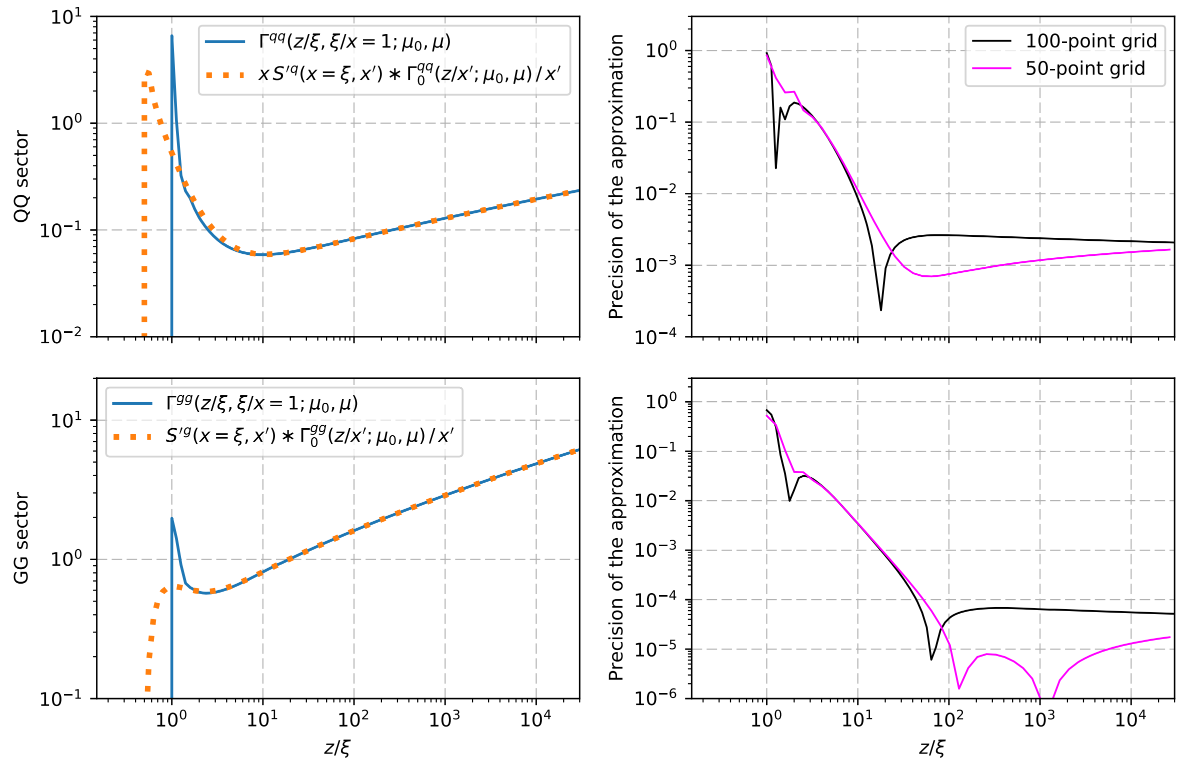

FIG. 8. Quality of the approximation of LO evolution operators $\Gamma^{ab}(z/\xi, \xi/x; \mu_0, \mu)$ by Eq. (16), as a function of z/ξ in the case where $\xi = x$, $\mu_0 = 1$ GeV and $\mu = 4.7$ GeV. The qq sector is displayed in upper-left panel while the gg sector in the lower-left panel. On the right, the relative precision of the approximation is given for two different discretizations of the evolution operators, either with 50 or 100 points. The dips in the curves correspond to a change of sign in the difference between the true value of the LO evolution operator and its approximation by Eq. (16).

sectors for $\xi = x$, where we expect the largest deviations between the DGLAP evolution operators and the GPD ones. In the region $z \gg \xi$, we observe a numerical agreement of the order of 10^{-3} for quarks and 10^{-4} for gluons. Using various discretizations of the evolution operators with the evolution code shows that numerical uncertainties dominate the discrepancy at large z. On the contrary, for $z \lesssim 10\xi$, both discretizations give generally similar results: in this region, the approximation of Eq. (16) gives significant discrepancies compared to the true value of the GPD evolution operator. It is obvious from the expression of S' in the Appendix that Eq. (16) cannot hold for small values of z: as can also be observed in Fig. 8, whereas the GPD evolution operator should be 0 for $z < \xi$ in the case where $x = \xi$, the rhs of Eq. (16) gives non-vanishing contributions down to $z = \xi/2$.

Under the assumption that the contribution of the region $z \lesssim 10\xi$, where the approximation of Eq. (16) is not very accurate, is negligible in the evolution of the GPD from μ_0 to μ, it is possible to write the right-hand side of (15) as

$$\mathcal{S}'^{a}(x,\xi,\mathbf{x}') * f^{a}(\mathbf{x}',\mu) = \mathcal{S}'^{a}(x,\xi,\mathbf{x}') * \sum_{b=q,g,\ldots} \int_0^1 \frac{\mathrm{d}z}{\mathbf{x}'} \Gamma_0^{ab}\left(\frac{z}{\mathbf{x}'};\mu_0,\mu\right) f^{b}(z,\mu_0) \tag{17}$$

$$\approx x^{p_a} \sum_{b=q,g,\ldots} \int_0^1 \frac{\mathrm{d}z}{x} \Gamma^{ab}\left(\frac{z}{\xi},\frac{\xi}{x};\mu_0,\mu\right) f^{b}(z,\mu_0), \tag{18}$$

where we used Eq. (5) in the first line and applied the approximation of Eq. (16) in the second. Since we assumed dominance of the $z \gtrsim 10\xi$ region in the integral over z, we can also assume that the skewness between incoming and outgoing four-momenta $z+\xi$ and $z-\xi$ is negligible, leading to the approximation that $f^b(z,\mu_0) \approx z^{-p_b} F^b(z,\xi,\mu_0)$. Hence,

$$\mathcal{S}'^{a}(x,\xi,\mathbf{x}') * f^{a}(\mathbf{x}',\mu) \approx x^{p_a} \sum_{b=q,g,\ldots} \int_0^1 \frac{\mathrm{d}z}{x} \Gamma^{ab}\left(\frac{z}{\xi},\frac{\xi}{x};\mu_0,\mu\right) \frac{F^{b}(z,\xi,\mu_0)}{z^{p_b}} \tag{19}$$

$$= F^{a}(x,\xi,\mu). \tag{20}$$

Therefore, the modeling strategy expressed in Eq. (15) relies on the same argument as the one presented before, that is, that there exists a lower scale μ_0 such that the large-z region dominates the evolution. However, any reference to μ_0 disappears in the final formulation of the proposal because the relation between general LO and DGLAP evolution operators of Eq. (16) holds independently of μ. However, the disappearance of μ_0 in the modeling strategy with the Shuvaev transform deprives us of a crucial tool to evaluate the uncertainty of the procedure.

Quantification of the systematic uncertainty of the Shuvaev procedure has been so far mostly treated with generic estimates, summarized as $\mathcal{O}(\xi^2)$ at LO and $\mathcal{O}(\xi)$ at NLO, based on considerations on the polynomial expansion of Gegenbauer moments of GPDs as functions of ξ [34]. The strict mathematical validity of these estimates has been criticized for instance in Refs. [41,69], where it is argued that, in general, truncating the ξ expansion of conformal moments—in this case to its first term—and performing their analytical continuation to apply the Shuvaev transform are noncommutative operations. Therefore, when the PDFs exhibit specific singularities, the reconstructed GPD would not produce the correct forward limit. Even assuming that the generic uncertainty estimates of $\mathcal{O}(\xi^2)$ at LO and $\mathcal{O}(\xi)$ at NLO are mathematically founded for most of the phenomenologically relevant parameterisations of PDFs, as argued in Ref. [70], it remains to clarify what is the actually size of these terms, which should at least depend on the hard scale μ. On the contrary, the uncertainty we have presented in the previous section does not scale as $\mathcal{O}(\xi^2)$ or $\mathcal{O}(\xi)$, and it is rather steady of the order of several percent to tens of percent at very small values of ξ.

Finally, the modeling with the Shuvaev transform is based on the property of LO evolution of conformal moments. It means that only the specific ξ dependence introduced by the LO evolution operator can be precisely reproduced, whereas our proposal can be straightforwardly extended to higher orders.

V. CONCLUSION

We propose a method to quantify the uncertainty in relating GPDs to PDFs at small x_B. This uncertainty estimate is generic and can be applied to any process involving GPDs in this kinematic regime. We observe that the uncertainty decreases quickly when the hard scale of the process increases but presents a mild dependence on the value of $\xi \approx x_B/2$, contrary to the typical estimates $\mathcal{O}(\xi^2)$ or $\mathcal{O}(\xi)$ provided in the literature. We suggest to apply our method to exclusive heavy-vector meson production, a hard process measured abundantly at small x_B. Assuming perturbative calculations starting from a scale as low as 1 GeV, a conservative estimate of the systematic uncertainty in relating the gluon GPD to the PDF is of the order of 10%–20% for J/ψ production if the hard scale 1.5 GeV is used [54,55] and of 2%–4% for Υ at a hard scale of 4.7 GeV. Starting perturbative evolution from a scale 1.4 GeV, we observe that the uncertainty for Υ is increased to 3%–8%, as the lever arm in evolution is reduced. The developed methodology is an important step to incorporate heavy-vector meson data into global PDF fits. We show that our method relies on the same general arguments as the one based on the Shuvaev transform.

We finally remark that deriving the ξ dependence of GPDs perturbatively from PDFs at small ξ effectively subtracts a degree of freedom to the modeling of GPDs in this kinematic domain. This entails a natural solution to the *deconvolution problem* of factorized observables. It has been explicitly demonstrated in Ref. [71] that for deeply virtual Compton scattering, a process closely related to HVMP, it is not possible to perform an extraction of GPDs from experimental data in a model-independent way at next-to-leading order due to the poor conditioning of the problem. The crux of the issue is essentially that the dimension of the space of kinematic variables available to experiments, (x_B, t, Q^2), is smaller than the space of variables of GPDs, (x, ξ, t, μ^2). This problem is considerably tamed by the procedure we propose in this article. The uncertainty on the extrapolation to vanishing skewness which we have derived represents then a measure of the systematic uncertainty associated to the choice of regularization that our procedure represents for the deconvolution problem at small ξ.

ACKNOWLEDGMENTS

We are grateful to M. Diehl for pointing out a mistake in Fig. 3. This work is supported in part by the European Unions Horizon 2020 research and innovation program under Grant Agreement No. 824093 and in the framework of the GLUODYNAMICS project funded by the "P2IO LabEx (ANR-10-LABX-0038)" in the framework "Investissements dAvenir" (ANR-11-IDEX-0003-01) managed by the Agence Nationale de la Recherche (ANR), France.

APPENDIX: FORMULAS FOR THE SHUVAEV TRANSFORM

The operator S'^a resulting from the composition of the Shuvaev operator S^a and the Mellin transform acts on a PDF $f^a(w)$ in the following way [34]:

$$\mathcal{S}'^a(x,\xi,\mathbf{x}') * f^a(\mathbf{x}') = \int_{-1}^{1} \mathrm{d}x' \left[\frac{2}{\pi}\mathrm{Im}\int_0^1 \mathrm{d}s \left(\frac{4s(1-s)}{(x+\xi(1-2s))^{1+p_a}} \times \sqrt{1-\frac{4sx'(1-s)}{x+\xi(1-2s)}}\right)^{-1}\right] \frac{\mathrm{d}}{\mathrm{d}x'}\left(\frac{f^a(x')}{|x'|}\right), \tag{A1}$$

where $p_a = 1$ for gluons ($a = g$) and 0 for quarks ($a = q$). A study of the support of the integral yields that, for $x > \xi > 0$, Eq. (A1) can be expressed as

$$\mathcal{S}'^a(x,\xi,\mathbf{x}') * f^a(\mathbf{x}') = \int_{x/2+\sqrt{x^2-\xi^2}/2}^{1} \mathrm{d}x' C^a(x,\xi,x') \times \frac{\mathrm{d}}{\mathrm{d}x'}\left(\frac{f^a(x')}{x'}\right), \tag{A2}$$

$$C^a(x,\xi,x') = \frac{2}{\pi}\mathrm{Im}\int_{s_1}^{s_2} \mathrm{d}s \left(\frac{4s(1-s)}{(x+\xi(1-2s))^{1+p_a}} \times \sqrt{1-\frac{4sx'(1-s)}{x+\xi(1-2s)}}\right)^{-1}, \tag{A3}$$

$$s_{1,2} = \frac{1}{2} + \frac{\xi}{4x'} \mp \frac{\sqrt{4x'^2+\xi^2-4xx'}}{4x'}. \tag{A4}$$

It is clear that the integral is finite if $x > \xi$ as we never get to integrate up to the problematic boundaries $s = 0$ and 1. For $x = \xi$,

$$C^a(x,x,x') = \frac{2x^{1+p_a}}{\pi}\mathrm{Im}\int_{x/2x'}^{1} \mathrm{d}s \left(\frac{s}{2^{p_a-1}(1-s)^{p_a}} \times \sqrt{1-\frac{2sx'}{x}}\right)^{-1}. \tag{A5}$$

Considering that $p_a = 0$ for quarks and 1 for gluons, we find

$$C^q(x,x,x') = \frac{x}{\pi}\mathrm{Im}\int_{x/2x'}^{1} \frac{\mathrm{d}s}{s\sqrt{1-\frac{2sx'}{x}}} \tag{A6}$$

$$= -\frac{2x}{\pi}\arctan\left(\sqrt{\frac{2x'}{x}-1}\right), \tag{A7}$$

$$C^g(x,x,x') = \frac{2x^2}{\pi}\mathrm{Im}\int_{x/2x'}^{1} \mathrm{d}s \frac{1-s}{s\sqrt{1-\frac{2sx'}{x}}} \tag{A8}$$

$$= 2xC^q(x,x,x') + 2\frac{x^3}{x'\pi}\sqrt{\frac{2x'}{x}-1}. \tag{A9}$$

[1] F. Gelis, E. Iancu, J. Jalilian-Marian, and R. Venugopalan, The color glass condensate, Annu. Rev. Nucl. Part. Sci. **60**, 463 (2010).
[2] A. Cooper-Sarkar, P. Mertsch, and S. Sarkar, The high energy neutrino cross-section in the Standard Model and its uncertainty, J. High Energy Phys. 08 (2011) 042.
[3] V. Bertone, R. Gauld, and J. Rojo, Neutrino telescopes as QCD microscopes, J. High Energy Phys. 01 (2019) 217.
[4] J. J. Ethier and E. R. Nocera, Parton distributions in nucleons and nuclei, Annu. Rev. Nucl. Part. Sci. **70**, 43 (2020).
[5] J. Gao, L. Harland-Lang, and J. Rojo, The structure of the proton in the LHC precision era, Phys. Rep. **742**, 1 (2018).
[6] R. Gauld, J. Rojo, L. Rottoli, and J. Talbert, Charm production in the forward region: Constraints on the small-x gluon and backgrounds for neutrino astronomy, J. High Energy Phys. 11 (2015) 009.
[7] R. Gauld, J. Rojo, L. Rottoli, S. Sarkar, and J. Talbert, The prompt atmospheric neutrino flux in the light of LHCb, J. High Energy Phys. 02 (2016) 130.
[8] M. V. Garzelli, S. Moch, O. Zenaiev, A. Cooper-Sarkar, A. Geiser, K. Lipka, R. Placakyte, and G. Sigl (PROSA Collaboration), Prompt neutrino fluxes in the atmosphere with PROSA parton distribution functions, J. High Energy Phys. 05 (2017) 004.
[9] O. Zenaiev, M. V. Garzelli, K. Lipka, S. O. Moch, A. Cooper-Sarkar, F. Olness, A. Geiser, and G. Sigl (PROSA Collaboration), Improved constraints on parton distributions using LHCb, ALICE and HERA heavy-flavour measurements and implications for the predictions for prompt atmospheric-neutrino fluxes, J. High Energy Phys. 04 (2020) 118.
[10] R. Abdul Khalek, R. Gauld, T. Giani, E. R. Nocera, T. R. Rabemananjara, and J. Rojo, nNNPDF3.0: Evidence for a modified partonic structure in heavy nuclei, Eur. Phys. J. C **82**, 507 (2022).
[11] J. Breitweg *et al.* (ZEUS Collaboration), Exclusive electroproduction of ρ^0 and J/ψ mesons at HERA, Eur. Phys. J. C **6**, 603 (1999).
[12] S. Chekanov *et al.* (ZEUS Collaboration), Exclusive photoproduction of J/ψ mesons at HERA, Eur. Phys. J. C **24**, 345 (2002).
[13] C. Adloff *et al.* (H1 Collaboration), Diffractive photoproduction of psi(2S) mesons at HERA, Phys. Lett. B **541**, 251 (2002).
[14] S. Chekanov *et al.*, Exclusive electroproduction of j/ψ mesons at HERA, Nucl. Phys. **B695**, 337 (2004).
[15] A. Aktas *et al.* (H1 Collaboration), Elastic J/ψ production at HERA, Eur. Phys. J. C **46**, 585 (2006).
[16] S. Chekanov *et al.* (ZEUS Collaboration), Measurement of J/ψ photoproduction at large momentum transfer at HERA, J. High Energy Phys. 05 (2010) 085.
[17] C. Alexa *et al.* (H1 Collaboration), Elastic and proton-dissociative photoproduction of J/ψ mesons at HERA, Eur. Phys. J. C **73**, 2466 (2013).
[18] R. Aaij *et al.* (LHCb Collaboration), Exclusive J/ψ and $\psi(2S)$ production in pp collisions at $\sqrt{s} = 7$ TeV, J. Phys. G **40**, 045001 (2013).
[19] R. Aaij *et al.* (LHCb Collaboration), Updated measurements of exclusive J/ψ and $\psi(2S)$ production cross-sections in pp collisions at $\sqrt{s} = 7$ TeV, J. Phys. G **41**, 055002 (2014).
[20] B. Abelev *et al.* (ALICE Collaboration), Exclusive J/ψ Photoproduction Off Protons in Ultra-Peripheral p-Pb Collisions at $\sqrt{s_{NN}} = 5.02$ TeV, Phys. Rev. Lett. **113**, 232504 (2014).
[21] R. Aaij *et al.* (LHCb Collaboration), Measurement of the exclusive Υ production cross-section in pp collisions at $\sqrt{s} = 7$ TeV and 8 TeV, J. High Energy Phys. 09 (2015) 084.
[22] R. Aaij *et al.* (LHCb Collaboration), Central exclusive production of J/ψ and $\psi(2S)$ mesons in pp collisions at $\sqrt{s} = 13$ TeV, J. High Energy Phys. 10 (2018) 167.
[23] A. M. Sirunyan *et al.* (CMS Collaboration), Measurement of exclusive Υ photoproduction from protons in pPb collisions at $\sqrt{s_{NN}} = 5.02$ TeV, Eur. Phys. J. C **79**, 277 (2019).
[24] P. Agostini *et al.* (LHeC, FCC-he Study Group Collaborations), The large hadron-electron collider at the HL-LHC, J. Phys. G **48**, 110501 (2021).
[25] Typical values of Bjorken's x_B are of the order of $e^{-y} m_V/\sqrt{s}$, where y is the pseudorapidity of the meson.
[26] R. Abdul Khalek *et al.*, Science requirements and detector concepts for the electron-ion collider: EIC Yellow Report, Nucl. Phys. **A1026**, 122447 (2022).
[27] D. Y. Ivanov, A. Schafer, L. Szymanowski, and G. Krasnikov, Exclusive photoproduction of a heavy vector meson in QCD, Eur. Phys. J. C **34**, 297 (2004); Eur. Phys. J. C **75**, 75(E) (2015).
[28] D. Müller, D. Robaschik, B. Geyer, F. M. Dittes, and J. Hořejši, Wave functions, evolution equations and evolution kernels from light ray operators of QCD, Fortschr. Phys. **42**, 101 (1994).
[29] X.-D. Ji, Gauge-Invariant Decomposition of Nucleon Spin, Phys. Rev. Lett. **78**, 610 (1997).
[30] X.-D. Ji, Deeply virtual Compton scattering, Phys. Rev. D **55**, 7114 (1997).
[31] A. Radyushkin, Asymmetric gluon distributions and hard diffractive electroproduction, Phys. Lett. B **385**, 333 (1996).
[32] A. V. Radyushkin, Nonforward parton distributions, Phys. Rev. D **56**, 5524 (1997).
[33] A. Shuvaev, Solution of the off forward leading logarithmic evolution equation based on the Gegenbauer moments inversion, Phys. Rev. D **60**, 116005 (1999).
[34] A. G. Shuvaev, K. J. Golec-Biernat, A. D. Martin, and M. G. Ryskin, Off diagonal distributions fixed by diagonal partons at small x and xi, Phys. Rev. D **60**, 014015 (1999).
[35] S. P. Jones, A. D. Martin, M. G. Ryskin, and T. Teubner, Probes of the small x gluon via exclusive J/ψ and Υ production at HERA and the LHC, J. High Energy Phys. 11 (2013) 085.
[36] C. A. Flett, S. P. Jones, A. D. Martin, M. G. Ryskin, and T. Teubner, How to include exclusive J/ψ production data in global PDF analyses, Phys. Rev. D **101**, 094011 (2020).
[37] C. A. Flett, S. P. Jones, A. D. Martin, M. G. Ryskin, and T. Teubner, Predictions of exclusive Υ photoproduction at the LHC and future colliders, Phys. Rev. D **105**, 034008 (2022).
[38] M. Diehl, Generalized parton distributions, Phys. Rep. **388**, 41 (2003).
[39] A. V. Belitsky and A. V. Radyushkin, Unraveling hadron structure with generalized parton distributions, Phys. Rep. **418**, 1 (2005).

[40] S. Boffi and B. Pasquini, Generalized parton distributions and the structure of the nucleon, Riv. Nuovo Cimento **30**, 387 (2007).

[41] M. Diehl and W. Kugler, Some numerical studies of the evolution of generalized parton distributions, Phys. Lett. B **660**, 202 (2008).

[42] M. Burkardt, Impact parameter dependent parton distributions and off forward parton distributions for zeta—> 0, Phys. Rev. D **62**, 071503 (2000); Phys. Rev. D **66**, 119903(E) (2002).

[43] Y. L. Dokshitzer, Calculation of the structure functions for deep inelastic scattering and e+ e- annihilation by perturbation theory in quantum chromodynamics., Sov. Phys. JETP **46**, 641 (1977).

[44] V. N. Gribov and L. N. Lipatov, Deep inelastic e p scattering in perturbation theory, Sov. J. Nucl. Phys. **15**, 438 (1972).

[45] G. Altarelli and G. Parisi, Asymptotic freedom in parton language, Nucl. Phys. **B126**, 298 (1977).

[46] Following Eq. (2), $x^{-p_a}F^a(x,\xi,t,\mu)$, where $p_a = 1$ if $a = g$ and 0 otherwise, gives exactly the correct forward limit $f^a(x,\mu)$ whether $a = q$ or g.

[47] L. A. Harland-Lang, A. D. Martin, P. Motylinski, and R. S. Thorne, Parton distributions in the LHC era: MMHT 2014 PDFs, Eur. Phys. J. C **75**, 204 (2015).

[48] We use evolution equations with noninfinitesimal distance between μ_0 and μ. It is more frequent to see them obtained by applying $\mathrm{d}/\mathrm{d}\log\mu$ to Eq. (4). The differential form involves the derivative of Γ^{ab} with respect to μ, known as *splitting function*, which is a distribution involving Dirac δ functions and plus prescriptions. Using integrated evolution equations allows one to treat Γ^{ab} as an ordinary weighting function and not as a mathematical distribution (if $\mu \neq \mu_0$).

[49] L. Frankfurt, A. Freund, V. Guzey, and M. Strikman, Nondiagonal parton distribution in the leading logarithmic approximation, Phys. Lett. B **418**, 345 (1998); Phys. Lett. B **429**, 414(E) (1998).

[50] A. D. Martin and M. G. Ryskin, The effect of off diagonal parton distributions in diffractive vector meson electroproduction, Phys. Rev. D **57**, 6692 (1998).

[51] V. Bertone, S. Carrazza, and J. Rojo, APFEL: A PDF evolution library with QED corrections, Comput. Phys. Commun. **185**, 1647 (2014).

[52] V. Bertone, APFEL++: A new PDF evolution library in C++, Proc. Sci. DIS2017 (**2018**) 201.

[53] V. Bertone, H. Dutrieux, C. Mezrag, J. M. Morgado, and H. Moutarde, Revisiting evolution equations for generalised parton distributions, Eur. Phys. J. C **82**, 888 (2022).

[54] S. P. Jones, A. D. Martin, M. G. Ryskin, and T. Teubner, Exclusive J/ψ and Υ photoproduction and the low x gluon, J. Phys. G **43**, 035002 (2016).

[55] S. P. Jones, A. D. Martin, M. G. Ryskin, and T. Teubner, The exclusive J/ψ process at the LHC tamed to probe the low x gluon, Eur. Phys. J. C **76**, 633 (2016).

[56] This region is sometimes referred to as the DGLAP region, due to the fact that the GPD evolution equations for $\xi \leq x$ shares many similarities with the DGLAP evolution equations. On the contrary, the region where $\xi \geq x$ is called Efremov-Radyushkin-Brodsky-Lepage (ERBL) thanks to a parallel with the ERBL evolution equations for distribution amplitudes [66,72]. We do not use these appellations to reserve the term DGLAP to the sole evolution equations for PDFs.

[57] N. Chouika, C. Mezrag, H. Moutarde, and J. Rodríguez-Quintero, Covariant Extension of the GPD overlap representation at low Fock states, Eur. Phys. J. C **77**, 906 (2017).

[58] N. Chouika, C. Mezrag, H. Moutarde, and J. Rodríguez-Quintero, A Nakanishi-based model illustrating the covariant extension of the pion GPD overlap representation and its ambiguities, Phys. Lett. B **780**, 287 (2018).

[59] I. V. Anikin and O. V. Teryaev, Dispersion relations and subtractions in hard exclusive processes, Phys. Rev. D **76**, 056007 (2007).

[60] M. Diehl and D. Y. Ivanov, Dispersion representations for hard exclusive processes: Beyond the Born approximation, Eur. Phys. J. C **52**, 919 (2007).

[61] I. V. Musatov and A. V. Radyushkin, Evolution and models for skewed parton distributions, Phys. Rev. D **61**, 074027 (2000).

[62] R. D. Ball, V. Bertone, F. Cerutti, L. Del Debbio, S. Forte, A. Guffanti, J. I. Latorre, J. Rojo, and M. Ubiali (NNPDF Collaboration), Reweighting NNPDFs: The W lepton asymmetry, Nucl. Phys. **B849**, 112 (2011); Nucl. Phys. **B854**, 926(E) (2012); Nucl. Phys. **B855**, 927(E) (2012).

[63] R. D. Ball, V. Bertone, F. Cerutti, L. Del Debbio, S. Forte, A. Guffanti, N. P. Hartland, J. I. Latorre, J. Rojo, and M. Ubiali, Reweighting and unweighting of parton distributions and the LHC W lepton asymmetry data, Nucl. Phys. **B855**, 608 (2012).

[64] H. Dutrieux, V. Bertone, H. Moutarde, and P. Sznajder, Impact of a positron beam at JLab on an unbiased determination of DVCS Compton form factors, Eur. Phys. J. A **57**, 250 (2021).

[65] R. D. Ball, V. Bertone, M. Bonvini, S. Marzani, J. Rojo, and L. Rottoli, Parton distributions with small-x resummation: evidence for BFKL dynamics in HERA data, Eur. Phys. J. C **78**, 321 (2018).

[66] A. V. Efremov and A. V. Radyushkin, Factorization and asymptotical behavior of pion form-factor in QCD, Phys. Lett. B **94**, 245 (1980).

[67] Y. M. Makeenko, Conformal operators in quantum chromodynamics, Sov. J. Nucl. Phys. **33**, 440 (1981).

[68] J. D. Noritzsch, Off forward parton distributions and Shuvaev's transformations, Phys. Rev. D **62**, 054015 (2000).

[69] K. Kumericki and D. Mueller, DVCS and the skewness effect at small x, in *Proceedings of the17th International Workshop on Deep-Inelastic Scattering and Related Subjects* (2009), p. 170, arXiv:0907.1207.

[70] A. D. Martin, C. Nockles, M. G. Ryskin, A. G. Shuvaev, and T. Teubner, Generalised parton distributions at small x, Eur. Phys. J. C **63**, 57 (2009).

[71] V. Bertone, H. Dutrieux, C. Mezrag, H. Moutarde, and P. Sznajder, Deconvolution problem of deeply virtual Compton scattering, Phys. Rev. D **103**, 114019 (2021).

[72] G. P. Lepage and S. J. Brodsky, Exclusive processes in quantum chromodynamics: Evolution equations for hadronic wave functions and the form-factors of mesons, Phys. Lett. **87B**, 359 (1979).